6422 *Macromolecules* **2010**, *43*, 6422–6428
DOI: 10.1021/ma1010167

Macromolecules
ARTICLE

Synthesis, Cocrystallization, and Microphase Separation of All-Conjugated Diblock Copoly(3-alkylthiophene)s

Jing Ge, Ming He, Feng Qiu,* and Yuliang Yang

The Key Laboratory of Molecular Engineering of Polymers, Ministry of Education, Department of Macromolecular Science, Fudan University, Shanghai 200433, China

Received May 6, 2010; Revised Manuscript Received July 2, 2010

ABSTRACT: A series of all-conjugated diblock copoly(3-alkylthiophene)s with varying alkyl chain length, poly(3-butylthiophene)-*b*-poly(3-hexylthiophene) (P3BT−P3HT), poly(3-butylthiophene)-*b*-poly(3-dodecylthiophene) (P3BT−P3DDT), and poly(3-hexylthiophene)-*b*-poly(3-dodecylthiophene) (P3HT−P3DDT), were synthesized by modified Grignard metathesis polymerization. The obtained diblock copoly(3-alkylthiophene)s have well-controlled block ratios and molecular weights with narrow polydispersity indices. The diblock copoly(3-alkylthiophene)s comprised by the blocks with the alkyl side-chain length different by two carbon atoms (represented by P3BT−P3HT) have the ability of cocrystallizing into an uniform crystal domain, with the mutual interdigitation of the different side chains of the two blocks into a common interchain lamella. Other diblock copoly(3-alkylthiophene)s with the side chains different by more than two carbon atoms prefer to microphase separating into two crystal domains formed by the independent crystallization of each block. The AFM images revealed the characteristics of microphase-separated morphology in P3BT−P3DDT and P3HT−P3DDT diblock copoly(3-alkylthiophene)s.

Introduction

All-conjugated molecules have attracted great interest in recent years due to their promising applications in organic field-effect transistors (OFETs),[1−3] organic light-emitting diodes (OLEDs),[4−6] and organic photovoltaic cells (OPVs).[7−9] It has been enormously reported that the performance of these semiconducting polymers relies crucially on their morphology on the nanometer scale.[10,11] One of the elegant way to manipulate the nanoscale pattern is to develop block copolymers (BCPs) containing semiconducting polymer with excellent electronic properties such as poly(3-alkylthiophene)s (P3AT), since BCPs can allow the formation of well-defined one-, two-, or three-dimensional microphase-separated domains in nanoscale dimension,[12,13] driven by factors such as immiscibility or the crystallinity difference between the two segments. Indeed, synthesis, self-assembly, and properties of rod−coil BCPs containing a conjugated rod-like block and a coil-like nonconjugated block have been extensively studied.[14−19] For example, Dai et al. reported that poly(3-hexylthiophene)-*b*-poly(2-vinylpyridine) (P3HT−P2VP) with low molecular weight can self-assemble into sphere, lamellae, hexagonal cylinder, and nanofiber gradually as the weight fraction of P3HT increases.[14] Iovu et al. reported that BCPs containing poly(3-hexylthiophene) (P3HT) as the rod block and polystyrene (PS), polyisoprene (PI), or various poly(methacrylates) (PMAs) as the coil block exhibit nanofibrillar morphology when cast from toluene solution.[17,18] Although the coil blocks can support the self-assembly and improve the mechanical properties, the introduction of those insulating segments does not carry any electronically active function and would lead to the decline in total electronic properties. Iovu et al. figured out that the field-effect transistor mobility of poly(3-hexylthiophene)-*b*-poly(methacrylate) (P3HT−PMA) decreases as PMA content increases.[18] Thereby, the investigation of all-conjugated BCPs composed of blocks all taking electronically active function has profound significance in optimizing the polymer electronic devices.

Thus, the research of rod−rod BCPs has been strongly intensified in recent years. Many of these researches put emphasis on the highly crystalline, semiconducting poly(3-alkylthiophene)s rod−rod BCPs, due to their large charge carrier mobility, bandgap in the visible region of the spectrum, environmental stability, solution processability, and synthetic versatility.[20−25] Iovu et al. have already reported the synthesis of poly(3-hexylthiophene)-*b*-poly(3-dodecylthiophene) (P3HT−P3DDT) via Grignard metathesis polymerization (GRIM).[26] However, its physical properties including crystalline properties and microphase morphology remain to be fully investigated. Wu et al. reported the synthesis of crystalline−crystalline poly(3-butylthiophene)-*b*-poly(3-octylthiophene) (P3BT−P3OT) via a similar method as above and pointed out that the microphase separation of P3BT−P3OT results in two distinct crystalline domains with the lamellar structure.[27] Unfortunately, the polydispersity indices of the polymers in their report were relatively high (PDI = 1.60) due to the poor selectivity of activation by isopropylmagnesium chloride of 2,5-dibromo-3-butylthiophene and 2,5-dibromo-3-octylthiophene monomers, while the narrow PDI is necessary for the formation of clear microphase-separated nanopatterns.

Herein, we synthesized three categories of crystalline−crystalline all-conjugated diblock copoly(3-alkylthiophene)s, poly(3-butylthiophene)-*b*-poly(3-hexylthiophene) (P3BT−P3HT), poly(3-butylthiophene)-*b*-poly(3-dodecylthiophene) (P3BT−P3DDT), and poly(3-hexylthiophene)-*b*-poly(3-dodecylthiophene) (P3HT−P3DDT) with well-controlled molecular weight and narrow PDI of 1.2−1.3 via a modified GRIM method[28,29] to explore the crystalline nature and nanoscale morphology of these BCPs. The GRIM polymerization is a quasi-living chain-growth synthesis[26,30] and thereby enables molecular weight to be controlled by changing the molar ratio of monomers to Ni catalyst. The monomers used here were 2-bromo-5-iodo-3-butylthiophene,

*Corresponding author: Tel +86 21 55664036; Fax +86 21 65640293; e-mail fengqiu@fudan.edu.cn.

 Published on Web 07/16/2010

2-bromo-5-iodo-3-hexylthiophene, and 2-bromo-5-iodo-3-dodecylthiophene, which all have good selectivity of activation by isopropylmagnesium chloride and hence ensure the narrow PDI. Since the length and bulkiness of the side chains strongly influence the physical properties of poly(3-alkylthiophene)s (P3ATs), such as solubility, melting point,[31,32] crystallinity,[33,34] and charge carrier mobility,[35−39] the combination of different P3AT blocks into one BCP is expected to lead to the formation of intriguing physical properties, caused by the differences in melting point, solubility, and crystalline nature of these blocks. Our research revealed that in a slow cooling process these BCPs cocrystallized into a common interchain lamella with the mutual interpenetration of the different side chains when their alkyl side chains were different by two carbon atoms (P3BT−P3HT). However, when the side-chain length of the two blocks was different by more than two carbon atoms (P3BT−P3DDT and P3HT−P3DDT), cocrystallization did not happen, and two crystal domains composed of the interdigitation of each side chain were observed.

Experimental Section

Materials. The monomers 2-bromo-5-iodo-3-butylthiophene (M_1), 2-bromo-5-iodo-3-hexylthiophene (M_2), and 2-bromo-5-iodo-3-dodecylthiophene (M_3) were synthesized according to the literature.[28] Isopropylmagnesium chloride (2.0 M solution in THF) (*i*-PrMgCl) and [1,3-bis(diphenylphosphino)propane]-dichloronicke(II) (Ni(dppp)Cl_2) were purchased from Sigma-Aldrich, and the other reagents and solvents were purchased from Sinopharm Chemical Reagent Co., Ltd. (SRC). Tetrahydrofuran (THF) was distilled from sodium benzophenone ketyl, and all other reagents and solvents were used as received.

General Aspects on the Synthesis of Diblock Copoly(3-alkylthiophene)s. All polymerizations were carried out in dry THF solvent and under the non-water and non-oxygen atmosphere. Monomer concentrations were typically 0.1 M. The molar ratio of Grignard reagent (*i*-PrMgCl) to the monomers was 1:1. All activation reactions of Grignard reagent were carried out at 0 °C. The molecular weight was controlled by fixing the ratio of the amount of Ni catalyst to the total monomer amount at 1:100. All polymerizations were carried out at 35 °C. All polymerizations were terminated by adding hydrogen chloride aqueous solution (aqueous HCl, 50 wt %), and the products were precipitated in methanol. The resulting polymer precipitates were filtered and successively washed by Soxhlet extraction using methanol and hexane and finally extracted using chloroform. The solvent was removed by evaporation to give a purple solid.

Synthesis of Poly(3-butylthiophene)-*b*-poly(3-hexylthiophene) (P3BT−P3HT). The molar feed ratios of M_1 to M_2 in the polymerization of P3BT−P3HT BCPs were 2:1, 1:1, and 1:2. The typical synthesis procedure of the P3BT−P3HT BCP with the feed molar ratio of 1:1 was as follows: two round-bottom flasks with side tubes (flask A and B) were dried by heating under reduced pressure and cooled to room temperature. M_1 (1.38 g, 4 mmol) was added into flask A under N_2 and then evacuated under reduced pressure to remove water and oxygen inside. After adding dry THF (40 mL) into the flask via a syringe, the solution was stirred at 0 °C. A 2.0 M solution of *i*-PrMgCl in THF (2 mL, 4 mmol) was added via a syringe, and the mixture was stirred at 0 °C for 30 min. Then the solution in flask A was heated up to 35 °C and followed by the addition of Ni(dppp)Cl_2 catalyst (43.38 mg, 0.08 mmol). The resulting mixture was stirred at 35 °C for 1 h. Meanwhile, in flask B, M_2 (1.50 g, 4 mmol) was reacted with *i*-PrMgCl (2 mL, 4 mmol) at 0 °C for 30 min. After the 1 h reaction in flask A, the solution in flask B was added to flask A in one portion, and the resulting mixture was reacted at 35 °C for 7 h. The reaction was quenched by adding HCl(aq) (50 wt %), and the product was precipitated into methanol. The residue was filtered and successively washed by Soxhlet extraction using methanol and hexane and finally extracted using chloroform. The solvent was removed by evaporation give a purple solid (0.64 g, 53%). P3BT−P3HT BCPs with the molar ratios of 1:2 and 2:1 were synthesized in the same way to give the purple solid (0.64 g, 51% and 0.59 g, 50%, respectively) as the final product. On the basis of the ratio of the integration areas of the two peaks at 0.98 and 0.91 ppm assigned to the resonances of terminal methyl groups in butyl and hexyl side chains derived from ^{1}H NMR spectra, the actual molar ratios of the P3BT and P3HT blocks were calculated to be 36:64, 51:49, and 66:34, denoted as B36H64, B51H49, and B66H34, respectively.

B36H64: ^{1}H NMR ($CDCl_3$), δ (ppm): 6.98 (1 H), 2.83−2.78 (2 H), 1.72−1.68 (2 H), 1.49−1.34 (4.56 H), 0.98 (1.08 H), 0.91 (1.92 H).

B51H49: ^{1}H NMR ($CDCl_3$), δ (ppm): 6.98 (1 H), 2.83−2.79 (2 H), 1.70−1.67 (2 H), 1.49−1.34 (3.96 H), 0.98 (1.53 H), 0.91 (1.47 H).

B66H34: ^{1}H NMR ($CDCl_3$), δ (ppm): 6.98 (1 H), 2.83−2.79 (2 H), 1.72−1.68 (2 H), 1.49−1.34 (3.36 H), 0.98 (1.98 H), 0.91 (1.02 H).

Synthesis of Poly(3-butylthiophene)-*b*-poly(3-dodecylthiophene) (P3BT−P3DDT). The molar feed ratio of M_1 and M_3 in P3BT−P3DDT was 1:1. The polymerization of M_1 (1.38 g, 4 mmol) and M_3 (1.20 g, 4 mmol) was carried out in the same manner as above to give the object P3BT−P3DDT product of 0.84 g (54% yield). As shown in ^{1}H NMR spectra, the peaks observed at δ 0.98 and 0.87 ppm could be assigned to the resonance of the terminal methyl groups in butyl and dodecyl side chains, respectively. By the same method as above, the actual molar ratio of the P3BT and P3DDT blocks in P3BT−P3DDT BCP was calculated to be 54:46, denoted as B54DD46.

B54DD46: ^{1}H NMR ($CDCl_3$), δ (ppm): 6.98−6.96 (1 H), 2.83−2.79 (2 H), 1.71−1.67 (2 H), 1.49−1.34 (9.36 H), 0.98 (1.62 H), 0.87 (1.38 H).

Synthesis of Poly(3-hexylthiophene)-*b*-poly(3-dodecylthiophene) (P3HT−P3DDT). The molar feed ratio of M_2 and M_3 in P3HT−P3DDT was 1:1. Similarly, the synthesis of P3HT−P3DDT was carried out in the same manner as above from M_2 (1.50, 4 mmol) and M_3 (1.20 g, 4 mmol) to obtain the final P3HT−P3DDT product (0.88 g, 53% yield). In ^{1}H NMR spectra, the peaks observed at δ 0.91 and 0.87 ppm could be assigned to the resonance of the terminal methyl groups in hexyl and dodecyl side chains, respectively. Thus, derived from the ratio of the integration areas of these two peaks, the actual molar ratio of the P3HT and P3DDT blocks in P3HT−P3DDT BCP was calculated to be 46:54, denoted as H46DDT54.

H46DD54: ^{1}H NMR ($CDCl_3$), δ (ppm): 6.98−6.97 (1 H), 2.80 (2 H), 1.72−1.69 (2 H), 1.44−1.34 (8.48 H), 0.91 (1.38 H), 0.87 (1.62 H).

Synthesis of Homopolymers. Poly(3-butylthiophene) (P3BT), poly(3-hexylthiophene) (P3HT), and poly(3-dodecylthiophene) (P3DDT) were also synthesized in the similar way except the addition of a second monomer. The typical synthesis procedure exemplified by P3BT was as follows: M_1 (2.76 g, 8 mmol) was added into a predried round-bottom flash with side tubes and then evacuated under reduced pressure to remove water and oxygen inside. After the addition of dry THF (80 mL), the solution was stirred at 0 °C, and then 2 M solution of *i*-PrMgCl in THF (4 mL, 8 mmol) was added via a syringe followed by stirring at 0 °C for 30 min. Subsequently, Ni(dppp)Cl_2 catalyst (43.38 mg, 0.08 mmol) was added in one portion, and the obtained mixture was reacted at 35 °C for 8 h. The reaction was quenched by adding HCl(aq) (50 wt %), and the product was precipitated into methanol. The residue was filtered and successively washed by Soxhlet extraction using methanol and hexane and finally extracted using chloroform. The solvent was removed by evaporation to give a purple solid.

Characterization. ^{1}H NMR spectra in $CDCl_3$ were collected on a DMX 500 MHz spectrometer using tetramethylsilane (TMS) as the internal standard. Gel permeation chromatography (GPC) was operated using a Agilent 1100 system equipped

with a UV detector (eluent: THF; calibration: polystyrene standards). UV−vis absorption spectra were recorded on Perkin-Elmer Lambda 35 UV−vis spectrophotometers. Differential scanning calorimetry (DSC) was performed using TA DSC Q2000 at a heating rate of 5 °C/min under N_2 flow. X-ray diffraction (XRD) data were recorded by a PANalytical X'Pert PRO X-ray diffractometer using Cu Kα radiation (λ = 1.541 Å) operating at 40 kV and 40 mA.

Film Preparation. Thick films of the homopolymers and diblock copoly(3-alkylthiophene)s for XRD measurements were first drop cast from 10 mg/mL chloroform solutions on precleaned 24 × 24 mm^2 glass slides. The films were then treated in the slow cooling process under argon flux: first melt at the temperature higher than their melting points for 15 min and then cooled to the room temperature at the rate of 5 °C/min. B36H64, B51H49, and B66H34 were melts at 280 °C; B54DD46 was melt at 260 °C, and H46DD54 was melt at 220 °C. Thin films of B51H49, B54DD46, and H46DD54 for AFM observations were first spin-coated from 10 mg/mL chloroform solutions onto Si substrate precleaned by piranha solution at the speed of 3000 rpm for 60 s at room temperature, then thermal annealed at 250, 230, and 200 °C for 30 min under the argon flux, respectively, and finally quenched to room temperature under argon flux.

Results and Discussion

Synthesis of Diblock Copoly(3-alkylthiophene)s. We used the modified GRIM method reported by Yokozawa et al.[28,29] to synthesize a series of diblock copoly(3-alkylthiophene)s, as illustrated in Scheme 1. First, the first block was polymerized with the Ni catalyst to obtain the end living P3AT polymers. Subsequently, a new portion of activated monomers was added to the reacting solution to obtain the final diblock copoly-(3-alkylthiophene)s.

Figure 1 shows the GPC profiles of P3ATs synthesized in the first step and the final diblock copoly(3-alkylthiophene)s after the second-stage polymerization. Compared to the peaks of the P3ATs obtained in the first stage, the peaks of the final diblock copoly(3-alkylthiophene)s all shift to a higher molecular weight with the maintenance of the single peak, indicating the production of the object BCPs with little P3ATs contaminant. These three categories of diblock copoly(3-alkylthiophene)s with different block ratios obtained here all show relatively high number-average molecular weight ($\bar{M}_n$) values of 13 100−18 600 and narrow PDI of 1.18−1.23, as shown in Table 1.

Scheme 1. Synthesis of Diblock Copoly(3-alkylthiophene)s Exemplified by Poly(3-butylthiophene)-*b*-poly(3-hexylthiophene) (P3BT−P3HT)

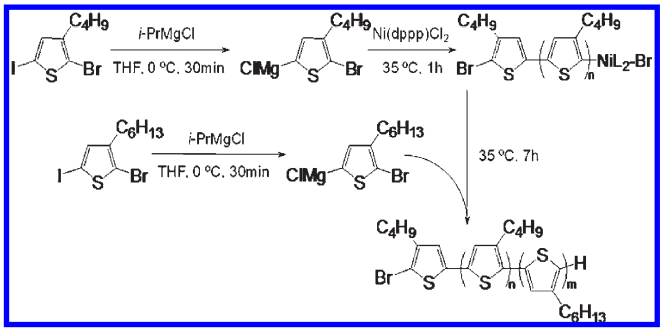

The compositions of the diblock copoly(3-alkylthiophene)s were determined from the ^{1}H NMR spectra (Figure S1). The triple peaks observed at δ 0.98, 0.91, and 0.87 ppm could be assigned to the resonance of terminal methyl groups in butyl, hexyl, and dodecyl side chains, respectively. The integration ratios of the peaks were consistent with the feed molar ratio of the two species in diclock copoly(3-alkylthiophene)s. These data are presented in Table 1. Take P3BT−P3HT as an example; from the ratio of the integration of the peaks at 0.98 and 0.91 ppm, the actual molar ratios of the P3BT and P3HT fractions were 36:64, 51:49, and 66:34, respectively, denoted as B36H64, B51H49, and B66H34, which were very close to the feed molar ratios of 1:2, 1:1, and 2:1. The compositions of P3BT−P3DDT and P3HT−P3DDT were calculated in the same way to be 54:46 and 46:54, respectively, denoted as B54DD46 and H46DD54, which were also close to the feed molar ratio (1:1). The results demonstrated that the molar ratio of the two blocks in BCPs can be designed by the feed molar ratio of the two monomers, indicating the well-controlled synthesis of the object diblock copoly(3-alkylthiophene)s with tunable composition and narrow PDI, via the quasi-living modified GRIM method.

It is worth to note that P3ATs with shorter side chain were needed to be polymerized first in order to obtain the final BCPs with the object molar ratio of the two segments. The reason could be attributed to the less steric hindrance of the shorter side chain; that is to say, the less steric hindrance from the first block could make the subsequent connection of the second block more efficient. In addition, the monomer

Table 1. Summary of Compositions and Molecular Weights of Poly-(3-alkylthiophene)s and Diblock Copoly(3-alkylthiophene)s

polymer	denotation	feed molar ratio	*n*/*m* (%)[a]	$\bar{M}_n$	PDI
P3BT		1:0	100:0	14 100	1.20
P3HT		1:0	100:0	18 800	1.19
P3DDT		1:0	100:0	17 000	1.23
P3BT-P3HT	B36H64	1:2	36:64	15 100	1.21
	B51H49	1:1	51:49	17 700	1.23
	B66H34	2:1	66:34	14 300	1.23
P3BT−P3DDT	B54DD46	1:1	54:46	13 100	1.18
P3HT−P3DDT	H46DD54	1:1	46:54	18 600	1.21

[a] Determined by ^{1}H NMR. *n*, *m*: the molar amount of the first and the second block in the synthesized diblock copoly(3-alkylthiophene)s, respectively.

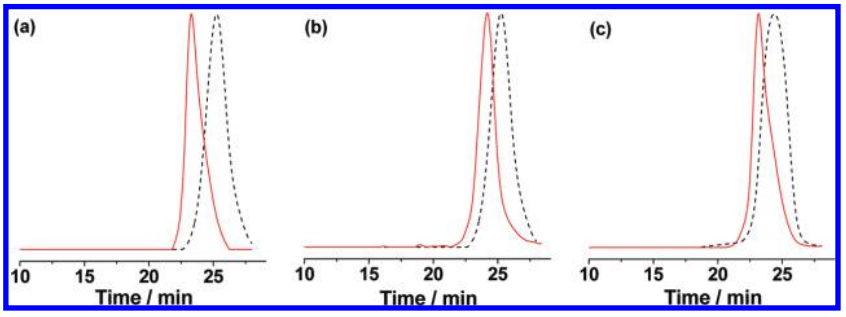

Figure 1. GPC profiles of diblock copoly(3-alkylthiophene)s. Dashed lines represent the GPC profiles of P3BT (a, b) and P3HT (c) synthesized in the first step and solid lines show the GPC profiles of the final B51H49 (a), B54DD46 (b), and H46DD54 (c) after the second-stage polymerization.

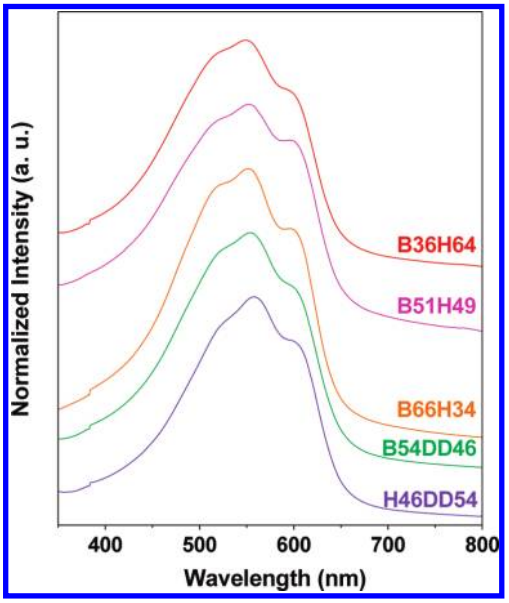

Figure 2. Normalized UV−vis absorption spectra of the films of all diblock copoly(3-alkylthiophene)s.

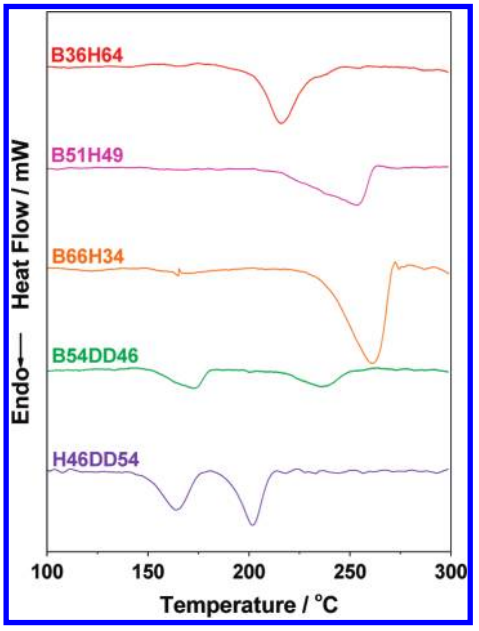

Figure 3. DSC endotherms of all the diblock copoly(3-alkylthiophene)s.

concentration of 2-bromo-5-iodo-3-butylthiohpene (M_2) should not be too high due to the solubility limitation of the P3BT block in THF. Thus, the concentration of M_2 in dry THF used here (0.1 M) is moderate.

UV−vis Absorption Spectra. To explore the photophysical properties of the diblock copoly(3-alkylthiophene)s, the UV−vis absorption spectra of the samples were measured. In the chloroform solution, all the diblock copoly(3-alkylthiophene)s showed an absorption peak at λ = 453 nm due to the intrachain $\pi-\pi^*$ transition of their main chain (these spectra are not shown here).[27] Figure 2 shows the absorption spectra of thin films of the diblock copoly(3-alkylthiophene)s drop-cast from chloroform solution. All of the diblock copoly(3-alkylthiophene)s films show the similar type of UV−vis absorption curve which has three peaks. The peaks at λ = 519−525 nm are attributed to the intrachain $\pi-\pi^*$ transition of the diblock copoly(3-alkylthiophene)s.[40] The peaks at λ = 550−558 nm come from the absorption of increased conjugation length due to the ordered stacking of the diblock copoly(3-alkylthiophene)s' backbones in films.[41] The shoulder peaks at λ = 600−602 nm result from the interchain $\pi-\pi$ interaction and their intensities are correlated with the degree of interchain order.[41,42] These results are very similar to the related poly(3-alkylthiophene) homopolymers.

Thermal Analysis. In order to investigate the crystalline behavior of the diblock copoly(3-alkylthiophene)s, all the polymers synthesized, including P3BT−P3HT with three different block ratios, P3BT−P3DDT, and P3HT−P3DDT, were characterized by DSC. All the samples were heated to 300 °C to eliminate the heat history, and the scan rate was 5 °C/min. Figure 3 shows the endothermic traces of the five diblock copoly(3-alkylthiophene)s. Their complete DSC traces and the complete DSC traces of the homopolymers are presented in Figures S2 and S3. The melting and crystallization temperatures of all these samples are summarized in Table 2. It is interesting to see that the P3BT−P3HT with the block ratios of 36:64, 51:49, and 66:34 all show a single endothermic peak with the melting points at 216, 253, and 248 °C, respectively. In contrast, B54DD46 and H46DD54 both show two distinct endothermic peaks with two melting points characteristic of the corresponding blocks (shown in Figure 3 and Table 2). For B54DD46, the two melting points are 235 and 173 °C, while H46DD54 has the melting points at 202 and 164 °C. The cooling thermograms also corroborate a single crystallization peak for P3BT−P3HT BCPs and two evident crystallization peaks for B54DD46 and H46DD54 (see Figure S2). These results indicate that the P3BT−P3HT BCPs undergo cocrystallization while B54DD46 and H46DD54 show microphase separation during the cooling processes of the DSC measurement. The cocrystallization in polymers is difficult, and only a few pairs have been reported to cocrystallize.[43−50] There are three requirements for cocrystallization: (1) structural similarity, (2) similar potential energies, and (3) almost similar crystallization kinetics.[51] P3ATs have a similar comb-like structure except the difference in alkyl side-chain length. According to the reported crystallization studies of P3ATs,[32,52] the enthalpies of fusion of ideal crystal and crystallization rates of P3ATs change with the varying side-chain length. The difference in enthalpy and crystallization rate of P3ATs increases with the increasing difference in alkyl side-chain length. Thereby, in our situation P3BT−P3HT BCPs are the best candidates for cocrystallization since their alkyl chain length only varies by two carbon atoms, while P3BT−P3DDT and P3HT−P3DDT BCPs are difficult to cocrystallize and usually prefer microphase separation. Additionally, the cocrystallization nature of P3BT−P3HT BCPs is not surprising, since the physical blends of poly(3-hexylthiophene)/poly(3-octylthiophene) would cocrystallize as reported by Pal et al.,[43−45] and

Table 2. Summary of DSC Measurements of Homopolymers and the Series of Diblock Copoly(3-alkylthiophene)s[a]

	T_m/°C		T_c/°C	
polymer	T_1	T_2	T_1	T_2
P3BT	261		220	
P3HT	222		194	
P3DDT	161		128	
B36H64	216		186	
B51H49	253		205	
B66H34	248		206	
B54DD46	235	173	192	128
H46DD54	202	164	176	138

[a] T_m: melting point; T_c: crystallization temperature.

Table 3. Summary of XRD Measurements of All the Homopolymers and the Diblock Copoly(3-alkylthiophene)s[a]

polymer	d_{100}/Å (2θ/deg)	
P3BT	12.3 (7.22)	
P3HT	15.9 (5.55)	
P3DDT	25.8 (3.43)	
B36H64	15.2 (5.81)	
B51H49	14.8 (5.99)	
B66H34	13.7 (6.47)	
B54DD46	22.1 (4.00)	12.8 (6.89)
H46DD54	25.1 (3.52)	16.6 (5.33)

[a] d_{100}: *d*-spacing of (100) plane in crystal lattice.

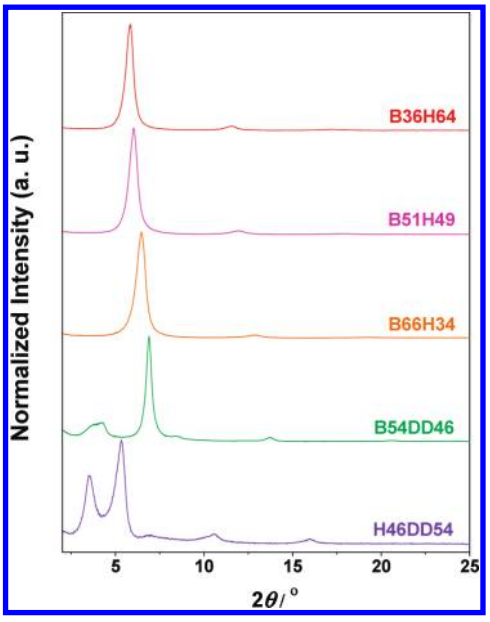

Figure 4. XRD profiles of the thick films of all diblock copoly(3-alkylthiophene)s.

Wu et al. have recently reported that random poly(3-butylthiophene-*co*-octylthiophene) with the alkyl chain length different by four carbon atoms can also cocrystallize.[53] It is worth to mention that when operated at the scan rate of 10 °C/min, B51H49 showed a strong melting peak and a shoulder peak at 259 and 237 °C, respectively (see Figure S2f), indicating that the cocrystallization behavior of P3BT−P3HT BCPs is favored thermodynamically. This is the reason why we set the scan rate at 5 °C/min.

XRD Studies. To further investigate the crystalline structures of the diblock copoly(3-alkylthiophene)s, thick films drop-cast from chloroform and treated in a slow cooling process (similar to the cooling process in DSC measurements) were characterized by XRD. The results obtained from the XRD measurements of all the homopolymers and the diblock copoly(3-alkylthiophene)s are summarized in Table 3. Figure 4 shows the XRD spectra of the thick films of the diblock copoly(3-alkylthiophene)s. In general, the XRD patterns of diblock copoly(3-alkylthiophene)s show the recognizable first-, second-, and third-order reflections from crystallographic (100), (200), and (300) planes. For example, the XRD scan of B51H49 film shows (100), (200), and (300) reflections at the 2θ angle of 5.99°, 12.0°, and 18.0°, respectively, and the (100) reflection corresponds to an interlayer d_{100} spacing of 14.8 Å of the well-organized lamellar structure. These results indicate that all the diblock copoly(3-alkylthiophene)s show a high degree of crystallinity and self-organized lamellar packing structure, comparable with P3ATs homopolymers[54] (shown in Figure S4).

Scheme 2. Schematic Representation of Cocrystalline Lamellar Structure of B51H49 Derived from XRD Results

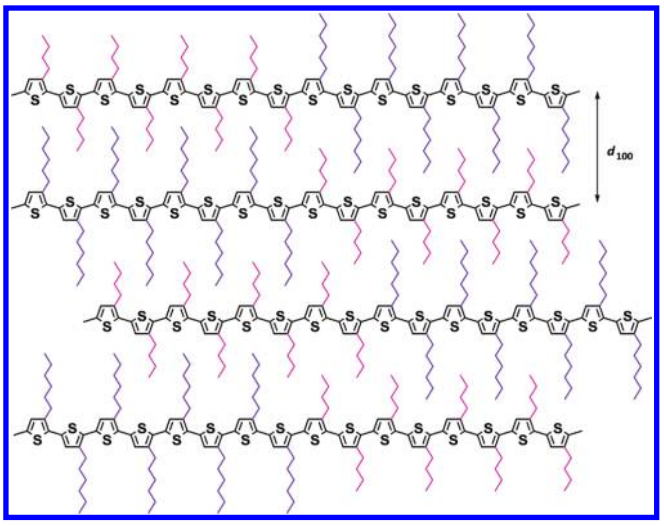

We note that the polymorphic behaviors of poly(3-alkylthiophene)s (P3ATs) have been studied at several instances.[33,55,56] Type 1 polymorph is common, while type 2 can also be formed when P3ATs undergo thermal and special solvent treatments[33,55] or decrease in their molecular weights.[56] However, until now there is no report on the polymorphic behaviors of diblock copoly(3-alkylthiophene)s. In our experiments, the samples were heated to melt state and then slowly cooled down; we did not observe the polymorph change according to the DSC and XRD measurements on the samples before and after the slow cooling treatment. Nonetheless, possible polymorphic changes in diblock copoly(3-alkylthiophene)s deserve a further investigation.

From the XRD scans in Figure 4 one can observe that B36H64, B51H49, and B66H34 all show one single sharp (100) diffraction peak at the 2θ angle of 5.81°, 5.99°, and 6.47°, respectively, corresponding to the d_{100} values of 15.2, 14.8, and 13.7 Å, respectively. And the d_{100} values progressively increase with the increasing content of the P3HT block. These results indicate that the diblock copoly(3-alkylthiophene)s with alkyl chain length different by two atoms could cocrystallize, as suggested by the above thermal analysis. Furthermore, the XRD measurement reveals that the cocrystals are formed by the cocrystallization of the two blocks into a common interchain lamella with the mutual interdigitation of the two different side chains to result in an uniform crystal domain. The ideal schematic representation of cocrystallization of P3BT−P3HT is shown in Scheme 2 exemplified by B51H49.

In contrast to P3BT−P3HT, B54DD46 shows two distinct (100) diffraction peaks at 4.00° and 6.89°, corresponding to the d_{100} values of 22.1 and 12.8 Å, respectively. The 22.1 Å spacing is characteristic of the interlayer stacking distance between P3DDT blocks in a lamellar packing structure (d_{P3DDT}), whereas the 12.8 Å spacing stems from the interlayer stacking distance between P3BT blocks (d_{P3BT}), indicating that B54DD46 microphase separated into two P3BT- and P3DDT-rich domains, and then each domain further crystallized independently. It is worthwhile to note that d_{P3DDT} is smaller than the d_{100} value (25.8 Å) of the P3DDT homopolymer, suggesting partial interdigitation between the dodecyl chain and/or the tilting of the side chain of P3DDT block in B54DD46. On the other hand, d_{P3BT} is very close to the d_{100} value (12.3 Å) of the P3BT homopolymer. Additionally, the (100) peak of P3DDT block is

Scheme 3. Schematic Representation of Microphase-Separated Lamellar Structure of B54DD46 with Two *d*-Spacing (d_{P3BT} and d_{P3DDT}) Derived from XRD Results, Which Has Already Been Pointed Out by Wu et al. Exemplified by Poly(3-butylthiophene)-*b*-poly(3-octylthiophene) (P3BT−P3OT)[27]

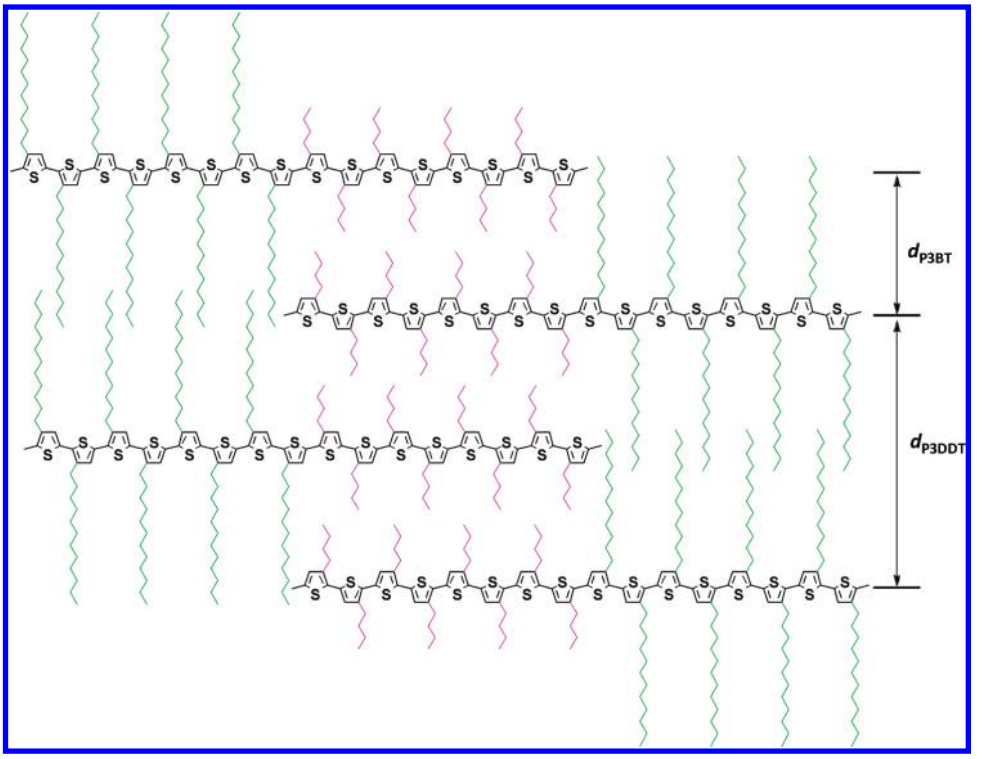

broad and weak, which is likely due to its imperfect crystallization affected by the prior crystallization of the P3BT block during the slow cooling process. This phenomenon indicate that the crystallization of P3BT is more favored thermodynamically than the crystallization of P3DDT, and the difference in crystallization between P3BT and P3DDT blocks might be the main reason that aroused the microphase separation in P3BT−P3DDT BCPs.

For H46DD54, the situation is similar; two distinct (100) diffraction peaks at 3.52° and 5.33° are observed, corresponding to the d_{100} values of 25.1 and 16.6 Å characteristic of P3DDT and P3HT blocks, respectively. This result also indicates the formation of the microphase separation of H46DD54 into two P3HT- and P3DDT-rich crystal domains. The schematic representation of microphase-separated lamellar structure is shown in Scheme 3. We note that such structure has already been pointed out by Wu et al. exemplified by poly(3-butylthiophene)-*b*-poly(3-octylthiophene) (P3BT−P3OT).[27]

Microphase Morphology. To investigate the microphase morphology of these diblock copoly(3-alkylthiophene)s, thin films of B51H49, B54DD46, and H46DD54 were prepared by spin-coating from 10 mg/mL chloroform solutions on Si substrate precleaned by piranha solution at room temeperature and then annealed at 250, 230, and 200 °C, respectively, under argon protection for 30 min. Their nanostructures were observed by AFM subsequently. Film thickness was estimated to be 40−50 nm (measured by AFM). Before the thermal annealing, observed using AFM, thin films of all these diblock copoly(3-alkylthiophene)s showed a flat surface without any phase pattern (not shown here). After the thermal annealing, B51H49 still showed a flat surface without any phase pattern (shown in Figure S5) due to its cocrystallization nature and hence resulting in one uniform phase. The situations were the same as B36H64 and B66H34; thus, their AFM images are not shown. Figure 5 shows the AFM images of B54DD46 and

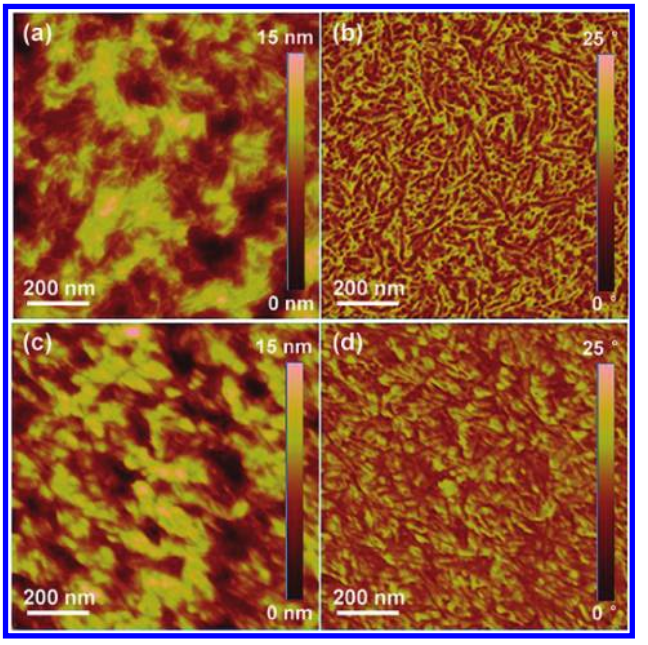

Figure 5. AFM height (a, c) and phase (b, d) images of thin films of B54DD46 after annealing at 230 °C (a, b) and H46DD54 after annealing at 200 °C (c, d) (image size: 1 × 1 μm^2).

H46DD54 after annealing. B54DD46 shows a clear nanopattern with partial lamellar-like structures and partial porous-like interconnected structures in its phase image (Figure 5b), while the height image shows a vague pattern (Figure 5a). The width of the structure is 10−19 nm, and H46DD54 shows a recognizable lamellar-like structures with the width in the range of 13−22 nm (Figure 5d), while the height image still remains vague (Figure 5c). The nanostructure observations of B54DD46 and H46DD54 are attributed to the microphase separation of the

two blocks in each of them. The somewhat blurred interfaces of H46DD54 may attribute to the similarity between the two blocks in crystallization that resulted in incomplete microphase-separated structures. In contrast, B54DD46 can produce nanopatterns with more distinguished interface, which enables poly(3-butylthiophene)-*b*-poly(3-dodecylthiophene) to be a more suitable model for the exploration of the nanoscale morphology of the rod−rod BCPs.

Conclusion

We have demonstrated the synthesis of a series of all-conjugated crystalline−crystalline diblock copoly(3-alkylthiophene)s with controlled molecular weight and narrow PDI via quasi-living GRIM polymerization. The DSC and XRD studies showed that the diblock copoly(3-alkylthiophene)s comprised by the blocks with the alkyl side-chain length different by two carbon atoms (represented by P3BT−P3HT) have the ability of cocrystallizing into an uniform crystal domain, with the mutual interdigitation of the different side chains of the two blocks into a common interchain lamella. Other diblock copoly(3-alkylthiophene)s with the side chains different by more than two carbon atoms prefer to microphase separating into two crystal domains formed by the independent crystallization of each block. The AFM images revealed the characteristics of microphase-separated morphology in P3BT−P3DDT and P3HT−P3DDT diblock copoly(3-alkylthiophene)s. A systematic study of dynamics of the nanostructure formation and carrier transport property in these all-conjugated diblocks is in progress.

Acknowledgment. We thank the financial support from the National Basic Research Program of China (Grant 2005CB623800) and National Natural Science Foundation of China (Grants 20625413, 20874021, and 20990231).

Supporting Information Available: ^{1}H NMR, complete DSC profiles, additional XRD scans, and AFM images. This material is available free of charge via the Internet at http://pubs.acs.org.

References and Notes

(1) Muccini, M. *Nature Mater*. **2006**, *5*, 605.
(2) Yamashita, Y. *Sci. Technol. Adv. Mater*. **2009**, *10*, 024313.
(3) Li, R. J.; Li, H. X.; Zhou, X. R.; Hu, W. P. *Prog. Chem*. **2007**, *19*, 325.
(4) Ikeda, H. *J. Photopolym. Sci. Technol*. **2008**, *21*, 327.
(5) Kudo, K.; Tanaka, S.; Iizuka, M.; Nakamura, M. *Thin Solid Films* **2003**, *438*, 330.
(6) Kitamura, M.; Imada, T.; Arakawa, Y. *Appl. Phys. Lett*. **2003**, *83*, 3410.
(7) Bernede, J. C. *J. Chil. Chem. Soc*. **2008**, *53*, 1549.
(8) Blom, P. W. M.; Mihailetchi, V. D.; Koster, L. J. A.; Markov, D. E. *Adv. Mater*. **2007**, *19*, 1551.
(9) Gunes, S.; Neugebauer, H.; Sariciftci, N. S. *Chem. Rev*. **2007**, *107*, 1324.
(10) Osaheni, J. A.; Jenekhe, S. A. *J. Am. Chem. Soc*. **1995**, *117*, 7389.
(11) Berresheim, A. J.; Muller, M.; Mullen, K. *Chem. Rev*. **1999**, *99*, 1747.
(12) Hamley, I. W. *Nanotechnology* **2003**, *14*, R39.
(13) Lee, M.; Cho, B. K.; Zin, W. C. *Chem. Rev*. **2001**, *101*, 3869.
(14) Dai, C. A.; Yen, W. C.; Lee, Y. H.; Ho, C. C.; Su, W. F. *J. Am. Chem. Soc*. **2007**, *129*, 11036.
(15) Ho, C. C.; Lee, Y. H.; Dai, C. A.; Segalman, R. A.; Su, W. F. *Macromolecules* **2009**, *42*, 4208.
(16) Leclere, P.; Hennebicq, E.; Calderone, A.; Brocorens, P.; Grimsdale, A. C.; Mullen, K.; Bredas, J. L.; Lazzaroni, R. *Prog. Polym. Sci*. **2003**, *28*, 55.
(17) Iovu, M. C.; Craley, C. R.; Jeffries-EL, M.; Krankowski, A. B.; Zhang, R.; Kowalewski, T.; McCullough, R. D. *Macromolecules* **2007**, *40*, 4733.
(18) Iovu, M. C.; Zhang, R.; Cooper, J. R.; Smilgies, D. M.; Javier, A. E.; Sheina, E. E.; Kowalewski, T.; McCullough, R. D. *Macromol. Rapid Commun*. **2007**, *28*, 1816.
(19) Jenekhe, S. A.; Chen, X. L. *Science* **1999**, *283*, 372.
(20) Sirringhaus, H.; Brown, P. J.; Friend, R. H.; Nielsen, M. M.; Bechgaard, K.; Langeveld-Voss, B. M. W.; Spiering, A. J. H.; Janssen, R. A. J.; Meijer, E. W.; Herwig, P.; de Leeuw, D. M. *Nature* **1999**, *401*, 685.
(21) Stutzmann, N.; Friend, R. H.; Sirringhaus, H. *Science* **2003**, *299*, 1881.
(22) Yang, H. C.; Shin, T. J.; Yang, L.; Cho, K.; Ryu, C. Y.; Bao, Z. N. *Adv. Funct. Mater*. **2005**, *15*, 671.
(23) Shrotriya, V.; Ouyang, J.; Tseng, R. J.; Li, G.; Yang, Y. *Chem. Phys. Lett*. **2005**, *411*, 138.
(24) Ren, G.; Wu, P. T.; Jenekhe, S. A. *Chem. Mater*. **2010**, *22*, 2020.
(25) Wu, P. T.; Ren, G.; Kim, F. S.; Li, C.; Mezzenga, R.; Jenekhe, S. A. *J. Polym. Sci., Polym. Chem*. **2010**, *48*, 614.
(26) Iovu, M. C.; Sheina, E. E.; Gil, R. R.; McCullough, R. D. *Macromolecules* **2005**, *38*, 8649–8656.
(27) Wu, P. T.; Ren, G. Q.; Li, C. X.; Mezzenga, R.; Jenekhe, S. A. *Macromolecules* **2009**, *42*, 2317.
(28) Yokoyama, A.; Miyakoshi, R.; Yokozawa, T. *Macromolecules* **2004**, *37*, 1169.
(29) Yokozawa, T.; Muroya, D.; Sugi, R.; Yokoyama, A. *Macromol. Rapid Commun*. **2005**, *26*, 979.
(30) Miyakoshi, R.; Yokoyama, A.; Yokozawa, T. *J. Am. Chem. Soc*. **2005**, *127*, 17542.
(31) Chen, S. A.; Ni, J. M. *Macromolecules* **1992**, *25*, 6081.
(32) Malik, S.; Nandi, A. K. *J. Polym. Sci., Polym. Phys*. **2002**, *40*, 2073.
(33) Prosa, T. J.; Winokur, M. J.; Moulton, J.; Smith, P.; Heeger, A. J. *Macromolecules* **1992**, *25*, 4364.
(34) Prosa, T. J.; Winokur, M. J.; McCullough, R. D. *Macromolecules* **1996**, *29*, 3654.
(35) Gartstein, Y. N.; Conwell, E. M. *Chem. Phys. Lett*. **1995**, *245*, 351.
(36) Dunlap, D. H.; Parris, P. E.; Kenkre, V. M. *Phys. Rev. Lett*. **1996**, *77*, 542.
(37) Novikov, S. V.; Dunlap, D. H.; Kenkre, V. M.; Parris, P. E.; Vannikov, A. V. *Phys. Rev. Lett*. **1998**, *81*, 4472.
(38) Kaneto, K.; Lim, W. Y.; Takashima, W.; Endo, T.; Rikukawa, M. *Jpn J. Appl. Phys*. **2000**, *39*, L872.
(39) Babel, A.; Jenekhe, S. A. *Synth. Met*. **2005**, *148*, 169.
(40) Kline, R. J.; McGehee, M. D.; Toney, M. F. *Nature Mater*. **2006**, *5*, 222.
(41) Li, L. G.; Lu, G. H.; Yang, X. N. *J. Mater. Chem*. **2008**, *18*, 1984.
(42) Brown, P. J.; Thomas., D. S.; Kohler, A.; Wilson, J. S.; Kim, J. S. *Phys. Rev. E* **2003**, *67*, 064203.
(43) Pal, S.; Nandi, A. K. *Macromolecules* **2003**, *36*, 8426.
(44) Pal, S.; Nandi, A. K. *Polymer* **2005**, *46*, 8321.
(45) Pal, S.; Nandi, A. K. *J. Appl. Polym. Sci*. **2006**, *101*, 3811–3820.
(46) Siracusa, V.; Gazzano, M.; Finelli, L.; Lotti, N.; Munari, A. *J. Polym. Sci., Polym. Phys*. **2006**, *44*, 1562.
(47) Jeong, Y. G.; Lee, J. H.; Lee, S. C. *Polymer* **2009**, *50*, 1559.
(48) Papageorgiou, G. Z.; Bikiaris, D. N. *Biomacromolecules* **2007**, *8*, 2437.
(49) Huang, Y. Y.; Nandan, B.; Chen, H. L.; Liao, C. S.; Jeng, U. S. *Macromolecules* **2004**, *37*, 8175.
(50) Vanhaecht, B.; Willem, R.; Biesemans, M.; Goderis, B.; Basiura, M.; Magusin, P. C. M. M.; Dolbnya, I.; Koning, C. E. *Macromolecules* **2004**, *37*, 421.
(51) Datta, J.; Nandi, A. K. *Polymer* **1994**, *35*, 4804.
(52) Causin, V.; Marega, C.; Marigo, A.; Valentini, L.; Kenny, J. M. *Macromolecules* **2005**, *38*, 409.
(53) Wu, P. T.; Ren, G.; Jenekhe, S. A. *Macromolecules* **2010**, *43*, 3306.
(54) Chen, T. A.; Wu, X. M.; Rieke, R. D. *J. Am. Chem. Soc*. **1995**, *117*, 233.
(55) Lu, G. H.; Li, L. G.; Yang, X. N. *Adv. Mater*. **2007**, *19*, 3594.
(56) Meille, S. V.; Romita, V.; Caronna, T.; Lovinger, A. J.; Catellani, M.; Belobrzeckaja, L. *Macromolecules* **1997**, *30*, 7898.